Evidence of A Possible Cycloaddition Channel in the Ethene + NO_3 Reaction

Rocío Cartas-Rosado,[†] María Esther Ruíz Santoyo,[‡] J. Raúl Alvarez-Idaboy,[‡] and Annik Vivier-Bunge*[,†]

Departamento de Química, Universidad Autónoma Metropolitana, Iztapalapa, 09340 México, D.F. México, and Gerencia de Ciencias del Ambiente, Instituto Mexicano del Petróleo, 07730 México, D.F. México

Received: April 30, 2001; In Final Form: July 2, 2001

In this work, the NO_3 addition to alkenes has been studied using ab initio quantum chemistry methods. In addition to the commonly accepted NO_3 radical addition to one of the C═C carbon atoms in alkenes, a symmetric transition state corresponding to the cycloaddition of the nitrate radical to the double bond has been identified, leading to the formation of a particularly stable NO_3-alkene cyclic radical. Consideration of the cyclic adduct is necessary to explain the formation of carbonyl products derived from the cleavage of the C═C bond in the absence of oxygen. Yet, the possibility of its formation from the nitroalkyl open adduct radical $R_1R_2C(ONO_2)CR_3R_4\cdot$ is hampered by the presence of a high energy barrier leading from the open to the cyclic adduct. The proposed cycloaddition channel is analogous to the Criegee mechanism for the cycloaddition of ozone to double bonds.

1. Introduction

Although the rates of the reactions of hydrocarbons with NO_3 radicals are generally more than a thousand times smaller than those with OH radicals, the former are important at nighttime, especially in urban atmospheres[1] where nitrogen oxides are present in large concentrations. In fact, it is presumed that NO_3 radicals drive the nighttime chemistry much in the same way as OH radicals drive the daytime chemistry of polluted atmospheres. Major products of the alkene + NO_3 reaction in the presence of molecular oxygen are organic nitrates and carbonyl compounds. In particular, for the propene + NO_3 reaction in the troposhere, toxic propylene glycol 1,2-dinitrate (PGDN) is known to be formed, together with nitroxyperoxypropyl nitrate (NPPN), 1-formylethylnitrate, formaldehyde, acetaldehyde, NO_2, and HNO_3.[2] It has been shown that organic nitrates might contribute significantly to the mutagenic activities observed in irradiated mixtures of hydrocarbons and nitrogen oxides.[3]

The kinetics and mechanisms of the gas-phase reactions of the NO_3 radical with alkenes have been reviewed and evaluated by Atkinson.[4] Room-temperature rate constants and Arrhenius parameters are available for a large number of alkenes, cycloalkenes and dienes.[4−7] In contrast with the negative activation energies observed in many radical addition reactions to double bonds, the addition of NO_3 to alkenes presents, in most cases, a normal Arrhenius behavior. Of the available data, the only rate constants which decrease (slightly) with temperature are those for *trans*-2-butene and α-pinene.[6] The recommended activation energies for the NO_3 addition to ethene, propene and 1-butene are 6.17, 2.3, and 1.88 kcal/mol,[6] respectively.

It has been assumed that, in the initial step, NO_3 adds to one of the carbon atoms of the double bond to form a nitroalkyl radical, $R_1R_2C(ONO_2)CR_3R_4\cdot$,[2,6] which, however, has not been identified experimentally. According to the Markownikoff rule, the radical electron is expected to be localized on the more substituted carbon atom.[8]

That the mechanism is electrophilic in nature is supported by the fact that the rate constant depends on the number of double bonds and their degree of substitution. Because values for the reaction rate constants are very similar at low and high pressures,[9] the process is believed to be irreversible. According to Dlugokencky and Howard,[9] the magnitude of the rate coefficients at room temperature indicates a reaction efficiency of about 1 in 100−1000 kinetic collisions for the NO_3 + olefin reactions. However, these authors note that the measured temperature dependencies give little insight into the origin of the low efficiencies, because different types of behavior are observed for different molecules. For example, *trans*-2-butene has a slightly curved Arrhenius plot, while isoprene has a small negative temperature coefficient and α-pinene has a small positive temperature coefficient. The magnitudes of the rate coefficients may be matched with reasonable models, but not the temperature dependencies.

It appears that the NO_3 + olefin reaction rate is determined by the rate of formation of the adduct. The reactions that follow the formation of the initial adduct are not well known. The product distribution varies with pressure, although the temperature dependence does not. Under atmospheric conditions, the nitroalkyl radical could react with O_2 to form a peroxyl radical, or with NO_2. Bandow et al.[2] have proposed a mechanism for NO_3 + propene, to explain the formation of PGDN as a final product. Measured and estimated yields for the products formed in the reactions of NO_3 with alkenes and dialkenes in 1 bar of synthetic air[10] indicate quite variable ratios of carbonyls to nitrate compounds. In an inert atmosphere the nitroalkyl radical probably rearranges to form an epoxide radical and NO_2. Epoxide compounds have indeed been obtained under these conditions.[11−13]

Theoretical calculations in general have been proved to be very useful to elucidate reaction mechanisms, inasmuch as all intermediates can be characterized regardless of their lifetimes. Nitrogen oxides, however, are known to be especially difficult

[†] Departamento de Química.
[‡] Gerencia de Ciencias del Ambiente.

10.1021/jp011631y CCC: $20.00 © 2001 American Chemical Society
Published on Web 09/14/2001

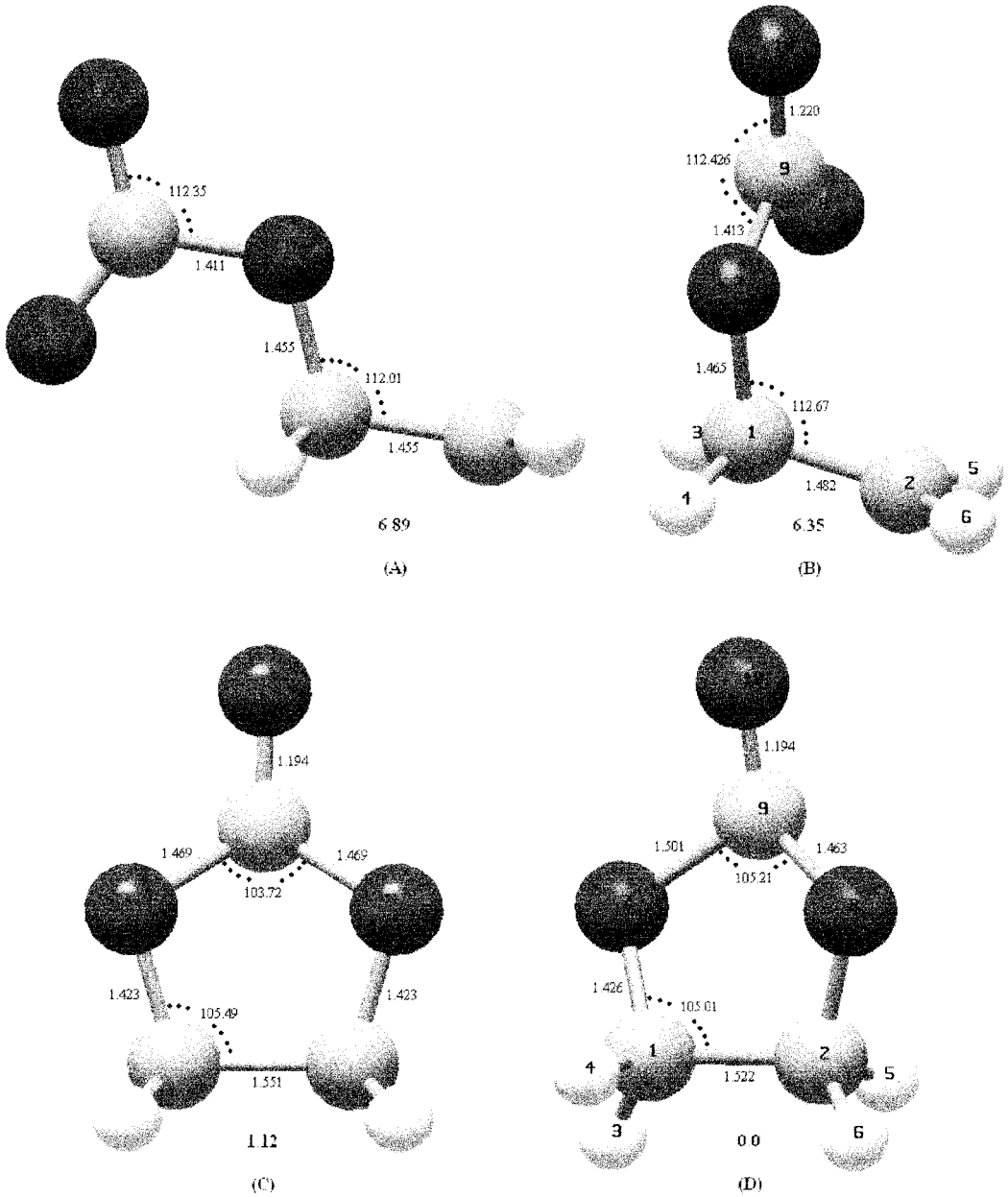

Figure 1. Optimized structures of the different conformers of the NO_3−ethene adduct. The PMP2 energies (in kcal/mol), relative to the most stable one (1D), are indicated below each structure.

to calculate. In fact, even very high level quantum chemistry methods do not agree on the symmetry of the ground state of NO_3.[6] To our knowledge, the only theoretical studies on the reaction of alkenes with the nitrate radical are those performed by Pérez-Casany et al. for ethene,[14] propene,[15] methyl substituted butene,[16] and haloalkenes[17,18] using the ROHF and the CAS-(SCF) methods in the first one, and density functional theory in the others. Their mechanism is compared with results of experimental studies at low pressures and temperatures in anaerobic conditions. After the addition of NO_3 to one of the carbon atoms, three pathways are proposed, the one leading to the formation of an epoxide being the one with the smallest activation energy.

There is still considerable uncertainty concerning the initial step in the NO_3 addition to a double bond. The CAS(SCF) calculations on ethene + NO_3[14] did not detect any structure between the reactants and the nitroalkyl adduct, and thus the 6.17 kcal/mol reported experimental activation barrier could not be reproduced. Later work by the same authors on other alkenes,[15−18] performed using the B3LYP density functional method, yielded a transition state whose reaction vector clearly corresponds to the formation of an O−C bond. Its energy, however, lies below the energy of the reactants, in disagreement with experimental results. This is a common problem with B3LYP calculations in bimolecular reactions.

In this work, an alternative mechanism is proposed, which involves the cycloaddition of NO_3 to the double bond. Cleavage of the cyclic adduct yields simple aldehydic products observed in the reaction with alkenes larger than ethene.[10] As explained by Barnes et al.,[10] the reaction of NO_3 with ethene is too slow to allow sufficient conversion of the reactant for a detailed product analysis. However, in this work, calculations have been performed with ethene because it is the simplest possible system of its kind. The mechanism is compared with the cycloaddition of ozone to double bonds.

Arrhenius parameters are calculated for both the addition to one of the carbon atoms and the cycloaddition, and compared with experimental results.

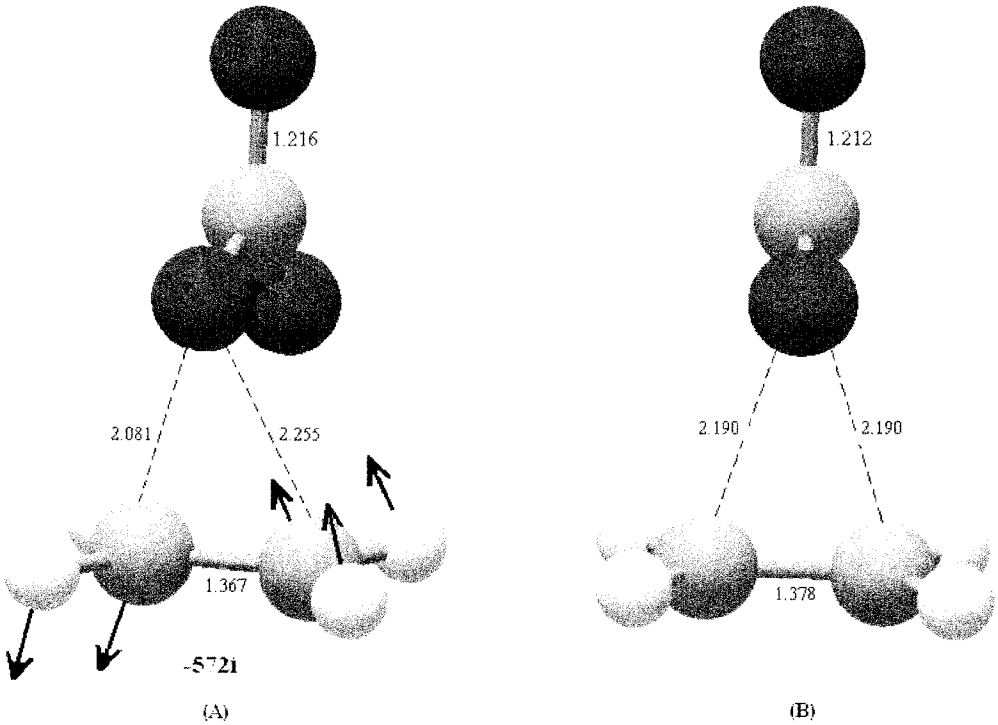

Figure 2. Optimized structure of the NO_3−ethene transition state (2A) and of the reactants complex (2B), along the reaction path leading to the formation of the open adduct. The main geometric parameters and the imaginary frequency are indicated, as obtained at the MP2/6-31G** level. The arrows indicate the motion of the transition vector.

TABLE 1: MP2/6-31G and B3LYP/6-31G** Geometrical Parameters of the Transition State Leading to the Formation of the Open Adduct**

parameter	MP2	B3LYP	parameter	MP2	B3LYP	parameter	MP2	B3LYP
$r(C_1C_2)$	1.3673	1.3563	$A(H_3C_1C_2)$	120.86	121.34	$D(H_3C_1C_2H_6)$	−178.056	178.755
$r(C_1H_3)$	1.0800	1.0848	$A(H_4C_1C_2)$	119.72	121.07	$D(H_4C_1C_2H_5)$	−178.232	−176.847
$r(C_1H_4)$	1.0783	1.0831	$A(H_5C_2C_1)$	121.11	121.56	$D(H_5C_2C_1H_3)$	−0.378	−4.094
$r(C_2H_5)$	1.0789	1.0854	$A(H_6C_2C_1)$	119.41	120.99	$D(H_6C_2C_1H_4)$	4.089	6.002
$r(C_2H_6)$	1.0776	1.0851	$A(O_7C_1C_2)$	78.68	94.98	$D(O_8N_9O_7C_1)$	−13.218	−9.637
$r(O_7C_1)$	2.0813	2.2689	$A(N_9O_7C_1)$	109.86	113.69	$D(O_{10}N_9O_7C_1)$	166.434	170.243
$r(O_7C_2)$	2.2550	2.7427	$A(O_{10}N_9O_7)$	116.08	112.19	$D(N_9O_7C_1C_2)$	91.496	89.835
$r(N_9O_7)$	1.3113	1.3274	$A(O_{10}N_9O_8)$	125.56	127.30	$D(O_{10}N_9O_8O_7)$	−179.616	−179.861
$r(N_9O_8)$	1.2503	1.2192	$A(O_8N_9O_7)$	118.35	120.50			
$r(O_{10}N_9)$	1.2158	1.2280						

2. Computational Methodology

Electronic structure calculations have been performed with the system of programs Gaussian98 (G98)[19] to study the NO_3 addition reaction to ethene. Unrestricted ab initio methods were used to calculate the energies of the radicals. Several methods were employed to introduce the correlation energy corrections, based on the Moller−Plesset perturbation theory, the coupled cluster method and on density functional theory.

All geometries were fully optimized at the MP2/6-31G(d,p) level and the character of the transition states was confirmed by a frequency calculation, performed at the same level, and presenting only one imaginary frequency corresponding to the expected transition vector. Projected MP2 energies were used in the calculation of the reaction energy profile, because it has been shown[21,22] that they give much better values for barriers. Zero point vibrational energy corrections (ZPE) at the MP2 level using the 6-31G(d,p) basis set were used in the calculation of the PMP2 activation energies and thermal correction energies at 298 K for the reaction energies.

Additional calculations were performed on the ethene + NO_3 reaction using other methods and basis sets to calculate the energies of the reactants and of the NO_3−ethene transition states in an effort to reproduce the experimental activation energy. The geometries of the reactants and of the transition states were reoptimized with the 6-311G** basis set. Frequencies were also calculated at this level to evaluate the influence of the basis. The CCSD(T)/6-311G** method was employed at the geometries optimized at the MP2/6-31G** level. The reactions were also studied by performing full geometry optimizations with the B3LYP method using the 6-31G** basis set.

The Arrhenius parameters were calculated at 298 K, using the CTST expression for the rate constant and the partition functions obtained from the Gaussian output. The latter have been corrected to account for internal rotations.[20]

3. Results and Discussion

At the beginning of this study on ethene + NO_3 using the MP2/6-31G(**) method, the usual assumption was made regarding the initial addition of the NO_3 radical to one of the carbon atoms of the double bond. Two different adducts were obtained, one of them corresponding to the nitrate radical pointing away from the double bond at an angle of 180° (Figure 1A), the other with the nitrate radical in a gauche position (Figure 1B). The latter was found to be slightly more stable. Structure 1B is very similar to the one reported by Pérez-Casany et al.[14] The NO_3 group has a planar geometry and lies in a plane

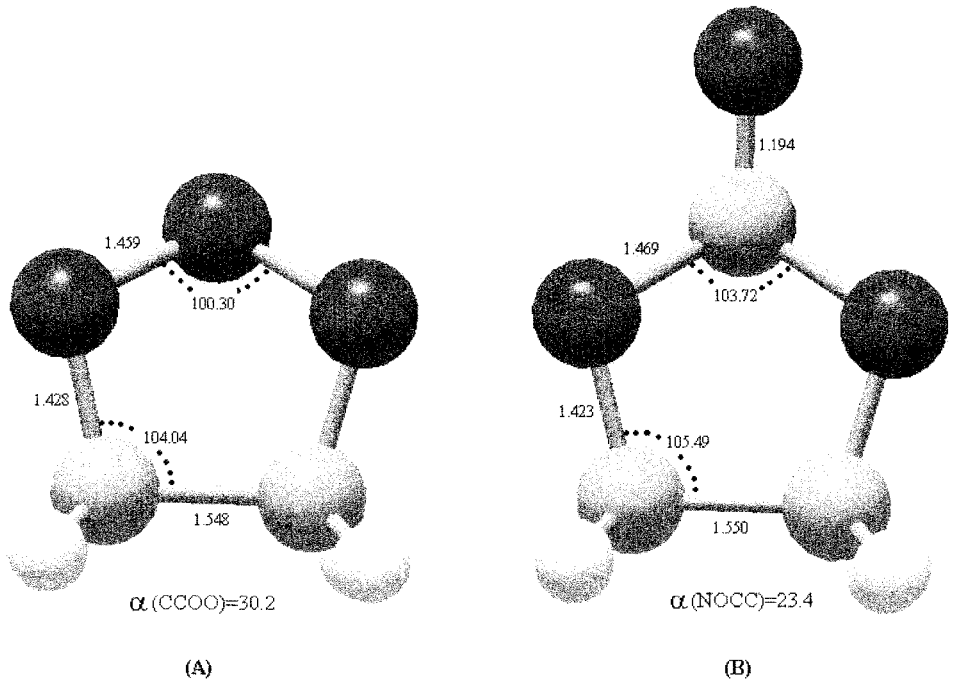

(A) (B)

Figure 3. Optimized structures of the O_3−ethene (A) and NO_3−ethene (B) cyclic adducts. The main geometric parameters are indicated, as obtained at the MP2/6-31G** level.

TABLE 2: MP2/6-31G and B3LYP/6-31G** Geometrical Parameters of the Cyclic Adduct**

parameter	MP2	B3LYP	parameter	MP2	B3LYP	parameter	MP2	B3LYP
$r(C_1C_2)$	1.5225	1.5369	$A(H_3C_1C_2)$	112.91	112.11	$D(H_3C_1C_2H_6)$	−89.838	−92.687
$r(C_1H_3)$	1.0882	1.0943	$A(H_4C_1C_2)$	110.92	111.03	$D(H_4C_1C_2H_5)$	161.188	155.484
$r(C_1H_4)$	1.0913	1.0969	$A(H_5C_2C_1)$	112.01	111.93	$D(H_5C_2C_1H_3)$	36.424	32.228
$r(C_2H_5)$	1.0915	1.0967	$A(H_6C_2C_1)$	113.45	112.94	$D(H_6C_2C_1H_4)$	34.925	30.569
$r(C_2H_6)$	1.0865	1.0913	$A(O_7C_1C_2)$	104.01	104.99	$D(O_7C_1C_2H_6)$	152.708	148.291
$r(O_7C_1)$	1.4263	1.4215	$A(O_8C_2C_1)$	102.48	103.42	$D(O_8C_2C_1O_7)$	37.867	32.634
$r(O_8C_2)$	1.4252	1.4198	$A(N_9O_7C_1)$	106.51	106.51	$D(N_9O_7C_1C_2)$	−17.512	−9.878
$r(N_9O_7)$	1.5009	1.5207	$A(N_9O_8C_2)$	103.33	103.20	$D(O_{10}N_9O_7C_1)$	−144.791	−146.452
$r(N_9O_8)$	1.4635	1.4717	$A(O_{10}N_9O_7)$	119.22	117.21	$D(O_{10}N_9O_8O_7)$	136.791	131.402
$r(O_{10}N_9)$	1.1940	1.2017	$A(O_{10}N_9O_8)$	118.97	117.05			
			$A(O_8N_9O_7)$	105.20	104.40			

which is almost perpendicular to the ethylene molecule. As already noted in ref 14, no stable van der Waals structure is found as reactants approach each other.

We investigated a large number of different channels for the approaching of the two molecules. A transition state structure was obtained, which, at the PMP2 level, lies 15.6 kcal/mol above the reactants and which has only one negative frequency at 573i cm^{-1}. It corresponds to a structure in which the plane of the NO_3 radical bisects the C═C bond, with one of the oxygen atoms approaching either one of the carbon atoms to form a C−O bond (Figure 2A). It is not symmetric: one of the C···O distances is considerably shorter than the other (2.081 and 2.255 Å, respectively). Its geometrical parameters obtained at the MP2/6-31G** level are given in Table 1. This structure is similar to the one obtained, for example, in ref 15, for propene, using the B3LYP-DFT method, and identified as the transition state for NO_3 addition. In this work, the equivalent structure was calculated in the case of ethene. When the B3LYP transition state was reoptimized with the MP2 method, a structure identical to the one shown in Figure 2A was obtained again.

An IRC calculation was performed at the same level to verify that the above transition state connects reactants and products. On the reactants' side, the IRC led to a new, stable, intermediate structure that is totally symmetric, with the two C···O distances equal to 2.1907 Å. It is shown in Figure 2B. Its energy is very close to that of the transition state, in fact only 0.17 kcal/mol lower, at the MP2 level. Thus, it appears that the potential energy surface is quite flat in the vicinity of the two structures (Figure 2A,B), which explains why it has been so difficult to obtain the MP2 transition state (2A) for the formation of the open adduct.[14]

In the course of further optimizing the adduct structure (1B), we performed rotations of the various torsion angles, and we eventually obtained a much more stable, symmetric structure which corresponds to a cyclic addition of NO_3 to the C═C bond (Figure 1C). In this system, the radical electron is clearly positioned on the terminal oxygen atom. At the PMP2 level, this structure is 6.35 kcal/mol more stable than the open gauche adduct. Additional optimization led to a slightly distorted cyclic structure (Figure 1D). The PMP2 energies of the four adducts are indicated in Figure 1, in kcal/mol, relative to the energy of the most stable one.

It is observed that the cyclic adduct in Figure 1C bears a striking resemblance to the primary ozonide obtained in the O_3 addition to ethene.[24] It has seven electrons more than the primary ozonide, but, because the unpaired electron in this radical structure does not contribute to the shared electrons in the cycle, the NO_3 + ethene cycloaddition could be viewed as being symmetry-allowed in the spirit of the $(4q + 2)$ Woodward−Hoffmann rules.[25] In Figure 3, the O_3−ethene and NO_3−ethene cyclic adducts are represented to show the similarities between both structures. The main geometric parameters are indicated,

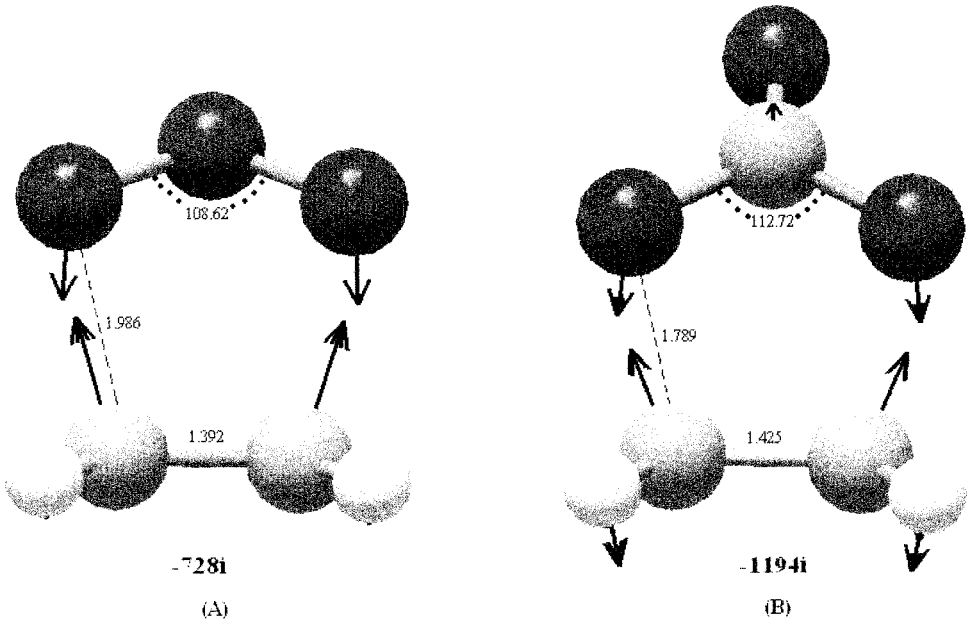

Figure 4. Optimized geometries of the O_3−ethene (A) and NO_3−ethene (B) transition states. The main geometric parameters and the imaginary frequencies are indicated, as obtained at the MP2/6-31G** level. The arrows indicate the motion of the transition vector.

as optimized at the MP2/6-31G** level. It can be seen that the geometry of the ethene group is practically the same in both adducts. The C−C bond is 1.55 Å in both, the C−O distance differs by less than 0.01 Å, and the OOO and ONO angles agree within 3°. Moreover, the dihedral angles indicating the position of the central O and N atoms with respect to the planarity of the five-membered rings are also quite close (NOCC = 23.4 and CCOO = 30.3). The geometrical parameters for the ethene + NO_3 cyclic adduct, obtained at the MP2/6-31G** level are given in Table 2.

A transition state analogous to the one obtained in the ozone addition by Anglada et al.[24] was investigated next and it was readily obtained. Again, a noticeable resemblance is observed between the ozone−ethene and the nitrate−ethene transition states. Both are shown in Figure 4, as calculated at the MP2/6-31G** level. In the NO_3 + ethene transition state, the oxygen atoms point at the carbon atoms, the nitrate radical approaching ethylene in a plane approximately parallel to it, with a C−O distance of 1.789 Å. In the O_3 + ethene case, the ozone moiety is also planar, and the C−O distance is larger, 1.986 Å, indicating an earlier transition state. In fact, both transition states occur closer to the reactants than to the products, but in the case of ozone, it can be seen that the C═C bond is a little shorter and closer to its value in ethene. The transition vectors clearly show the oxygen atoms of the ozone and of the nitrate groups, respectively, moving toward the carbon atoms (Figure 4). The imaginary frequencies are 728i and 1194i, respectively. The geometrical parameters for the ethene + NO_3 cyclic transition state, obtained at the MP2/6-31G** level are given in Table 3.

In the cycloaddition of ozone to ethene, a prereactive van der Waals complex has been identified, both experimentally, using microwave spectroscopy, and theoretically using MP4 ab initio calculations.[26] In line with our previous experience with radical additions to double bonds,[22,27−30] we assumed that such a van der Waals complex would be formed as the reactants, NO_3 and ethene, approached each other. Pérez-Casany et al.[14] had already searched the potential energy surface for such a minimum, with no success, and no complex was found in the present study either.

An explanation can be advanced in terms of electrostatic attractions. The orientation of the molecules in van der Waals

TABLE 3: MP2/6-31G Geometrical Parameters of the Cyclic Ethene-NO_3 Transition State**

parameter	MP2	parameter	MP2	parameter	MP2
$r(C_1C_2)$	1.4253	$A(H_3C_1C_2)$	118.56	$D(H_3C_1C_2H_6)$	149.227
$r(C_1H_3)$	1.0804	$A(H_4C_1C_2)$	118.86	$D(H_4C_1C_2H_5)$	−149.012
$r(C_1H_4)$	1.0792	$A(H_5C_2C_1)$	118.55	$D(H_5C_2C_1H_3)$	0.109
$r(C_2H_5)$	1.0804	$A(H_6C_2C_1)$	118.87	$D(H_6C_2C_1H_4)$	0.105
$r(C_2H_6)$	1.0792	$A(O_7C_1C_2)$	101.62	$D(O_7C_1C_2H_6)$	−104.304
$r(O_7C_1)$	1.7892	$A(O_8C_2C_1)$	101.64	$D(O_8C_2C_1O_7)$	0.155
$r(O_8C_2)$	1.7892	$A(N_9O_7C_1)$	102.90	$D(N_9O_7C_1C_2)$	−23.331
$r(N_9O_7)$	1.2895	$A(N_9O_8C_2)$	102.92	$D(O_{10}N_9O_7C_1)$	−121.750
$r(N_9O_8)$	1.2895	$A(O_{10}N_9O_7)$	122.83	$D(O_{10}N_9O_8O_7)$	165.906
$r(O_{10}N_9)$	1.2315	$A(O_{10}N_9O_8)$	122.84		
		$A(O_8N_9O_7)$	112.72		

complexes in general, clearly indicates that their formation is essentially determined by the long-range Coulombic interactions between the reactant molecules. In fact, in the prereactive complex formed between the OH radical and an unsaturated hydrocarbon, it is the H atom of the OH radical that points toward the π electrons of the double bond, even though the OH group has to flip over in order to form the C−O bond in the adduct.[21−23,27−30] In the case of ozone addition, the ozone molecule has a net dipole moment (0.6 D as calculated at the MP2 level), with a −0.1 charge on the terminal oxygen atoms. Thus, the latter are attracted to the positive hydrogen atoms in ethylene, while the central oxygen atom is drawn toward the π carbon−carbon bond. Experimentally, Gillies et al.[26] have found that their microwave data are consistent with a van der Waals structure having C_s symmetry, in which the nearly parallel planes of ethylene and ozone have a center of mass separation of 3.290 Å. The complex lies in a shallow minimum, with a binding energy of only 0.74 kcal/mol. In the case of the NO_3 radical in a D_{3h} conformation, however, there is no net dipole moment, and even if a slight deformation may occur when NO_3 approaches ethylene, the binding energy of the van der Waals complex would be too small for the complex to be observed.

The possibility of a cycloaddition mechanism in the NO_3 addition to alkenes which would resemble the cycloaddition mechanism of ozone has been considered by Atkinson[31] and by Canosa-Mas et al.[32] According to Atkinson's compilation[31] the rate constants for the reactions of OH with alkenes correlate

TABLE 4: Experimental Rate Constants k at 298 K (in cm^3 Molecule^{-1} s^{-1}) and Arrhenius Parameters, $k = Ae^{-B/T}$, (A in cm^3 Molecule^{-1} s^{-1}, B in K) for the Gas Phase Reaction of Ethene with OH, NO_3, and O_3[2]

OH			NO_3			O_3		
k	A	B	k	A	B	k	A	B
8.52×10^{-12}	1.96×10^{-12}	−438	2.05×10^{-16}	3.64×10^{-13}	3000	1.59×10^{-18}	9.14×10^{-15}	2580

TABLE 5: MP2/6-31G and B3LYP/6-31G** Geometrical Parameters of the Transition State Connecting the Open and the Cyclic Adducts**

parameter	MP2	B3LYP	parameter	MP2	B3LYP	parameter	MP2	B3LYP
$r(C_1C_2)$	1.4753	1.4853	$A(H_3C_1C_2)$	112.02	111.54	$D(H_3C_1C_2H_6)$	172.406	174.191
$r(C_1H_3)$	1.0869	1.0934	$A(H_4C_1C_2)$	114.46	113.43	$D(H_4C_1C_2H_5)$	−112.726	−107.663
$r(C_1H_4)$	1.0876	1.0944	$A(H_5C_2C_1)$	119.93	119.71	$D(H_5C_2C_1H_3)$	14.848	17.015
$r(C_2H_5)$	1.0765	1.0822	$A(H_6C_2C_1)$	119.03	119.15	$D(H_6C_2C_1H_4)$	44.831	49.511
$r(C_2H_6)$	1.0798	1.0851	$A(O_7C_1C_2)$	109.00	109.80	$D(O_8N_9O_7C_1)$	−18.582	−14.919
$r(O_7C_1)$	1.4922	1.4659	$A(N_9O_7C_1)$	108.02	108.95	$D(O_{10}N_9O_7C_1)$	146.742	145.132
$r(O_8C_2)$	1.9087	1.9641	$A(O_{10}N_9O_7)$	116.12	116.48	$D(N_9O_7C_1C_2)$	−21.258	−25.227
$r(N_9O_7)$	1.3853	1.4149	$A(O_{10}N_9O_8)$	130.32	128.07	$D(O_{10}N_9O_8O_7)$	−162.641	−157.175
$r(N_9O_8)$	1.2320	1.2713	$A(O_8N_9O_7)$	111.46	111.72			
$r(O_{10}N_9)$	1.2202	1.2238						

well with those for O(^{3}P) + alkene reactions, less well with those for NO_3 + alkene reactions and poorly with those for O_3 + alkene reactions, thus emphasizing the difference in mechanism. A comparison between the reactivity of NO_3 and that of O_3 was performed by Canosa-Mas et al.[32] by plotting the logarithms of the respective rate constants against each other, for a set of different alkenes, but they did not find a clear correlation. This could be taken as an indication of a competition between the open and the cycloaddition channels, the relative weights of the two channels being different for different alkenes.

Thus, the question which arises immediately is how does the cycloaddition channel compare, in energy, with the one corresponding to the formation of the open adduct. Also, the Arrhenius preexponential factor is expected to be much smaller in the cycloaddition. The experimental Arrhenius parameters for addition of OH, NO_3 and O_3 to ethene are presented in Table 4, as recommended by Atkinson.[4] A comparison between the preexponential factors of the three reactions shows that the NO_3 A-factor is intermediate between the other two.

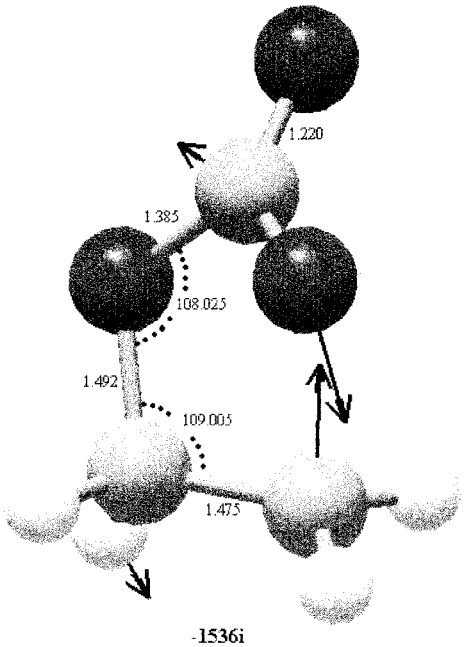

Figure 5. Optimized geometry of the transition state connecting the open and the cyclic adducts. The main geometric parameters and the imaginary frequency are indicated, as obtained at the MP2/6-31G** level. The arrows indicate the motion of the transition vector.

SCHEME 1

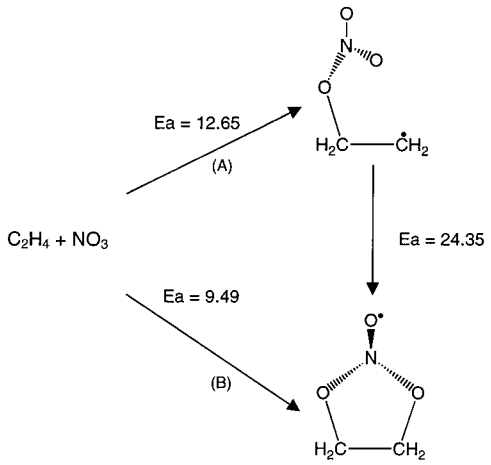

The calculations indicate that the PMP2 energy of the transition state (17.83 kcal/mol) is somewhat higher than the one corresponding to the open adduct transition state (15.6 kcal/mol). However, the zero point energy correction of the latter is considerably larger than the first, thus upsetting the order of the results. The corrected activation energies turn out to be 19.74 kcal/mol for the cyclic transition state, and 21.47 kcal/mol for the open transition state. Both are much too high if compared with the reported experimental values (5.71-6.21) kcal/mol).[7] In an effort to improve the values of the energy barriers, other methods were tested. The geometries of the reactants and of the transition states for the two channels were reoptimized with a larger basis set (6-311G**), and frequencies were also calculated at this level. No appreciable differences were observed in the size of the barriers, which were found to be even larger, 22.35 and 21.95 kcal/mol, for the cyclic and open channels, respectively. Thus, calculations with the 6-311G** basis set were not pursued further.

Single point CCSD(T) calculations at the MP2/6-31G** geometries were performed with the 6-311G** basis set. With this method, and using the MP2/6-31G** ZPE corrections, values of 9.49 and 12.65 kcal/mol were obtained for the cycloaddition and open adduct paths, respectively.

With the B3LYP/6-31G** method, only the transition state leading to the open adduct was obtained. It has an energy barrier of −0.37 kcal/mol. Negative barriers are often encountered when using B3LYP. Along the cyclic channel, a structure was found which has two imaginary frequencies, both at about −400 cm^{-1},

SCHEME 2

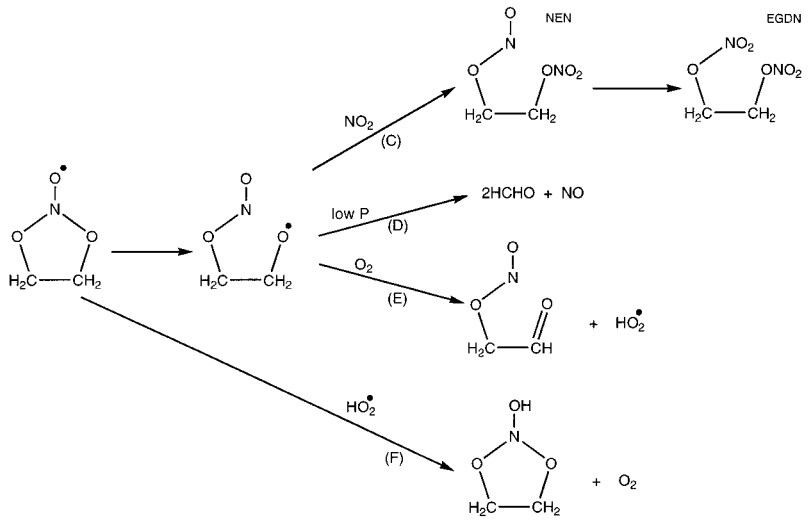

TABLE 6: Total Energies, ZPE, and TCE at 298 K (in hartrees) of the Reactants, Transition States, and Products in the NO_3 + Ethene Reaction

	PMP2/6-31G**[a]			B3LYP/6-31G**[a]	
	energy	ZPE (TCE)	CCSD(T)[a] energy	energy	ZPE (TCE)
ethene	−78.317282	0.052348 (0.055384)	−78.383805	−78.593807	0.051124 (0.054166)
NO_3	−279.530191	0.018176 (0.070524)	−279.665745	−280.216801	0.010684 (0.014708)
TS_{open}	−357.822519	0.079786 (0.085346)	−357.958864	−358.815621	0.066120 (0.07857)
TS_{cyclic}	−357.819056	0.073571 (0.078456)	−357.963894		
open adduct	−357.866907	0.070126 (0.076544)	−358.082774	−358.839961	0.068167 (0.074698)
cyclic adduct	−357.877039	0.074042 (0.079172)	−358.099674	−358.862634	0.071194 (0.076570)
$TS_{open \rightarrow cyclic}$	−357.819765	0.070965 (0.076000)	−358.044802	−358.813781	0.068190 (0.073420)

[a] The PMP2/6-31G** and B3LYP/6-31G** results correspond to total geometry optimization. The CCSD(T) energies are single point total energies obtained with the 6-311G** basis set at the MP2/6-31G** geometry.

one of them corresponding to the concerted approach of two oxygen atoms to the carbon atoms, the other being an oscillation of the nitrate group between the two carbon atoms. Refining this structure led to a true transition state in which only the second vibration is retained, i.e., it connects open adducts on either one of the carbon atoms. An unambiguous cyclic transition state could not be found with this method. Because the B3LYP method has often been shown to be unreliable for the calculation of transition states, in this work, it has been used mainly for comparison with Perez-Casany et al.'s work[14] and as a sometimes useful alternative when looking for difficult structures on the potential energy surface.

The preexponential factors for the cyclic and the open channels were calculated using the partition functions derived from frequency calculations with the MP2 method. The following *A* values are obtained: 7.55×10^7 L mol^{-1} s^{-1} for the open channel, and 3.03×10^6 L mol^{-1} s^{-1} for the cycloaddition. From a frequency calculation with the 6-311G** basis set, the results are similar: they are 7.16×10^7 and 2.99×10^6 L mol^{-1} s^{-1}, respectively. The experimental result recommended by Atkinson[4] is, in the same units, equal to 1.99×10^9. It is very interesting to note that the open channel does not yield a much larger preexponential factor than the cycloaddition. Actually, this is not unreasonable if one looks at the two transition states (Figures 2A and 4B). One can see that the open transition state is also quite constrained in the direction of the approach to the double bond, with the plane of the nitrate group approaching perpendicular to the ethene molecule and only one of the oxygen atoms pointing toward the double bond. Thus, the small energy difference between the transition states for channels A and B is expected to be compensated by the small difference in the *A* factors, and the rate constants could be similar. Indeed, using the CCSD(T) activation energies and the partition functions from the MP2/6-31G** frequency calculations, the rate constant coefficients estimated using the Arrhenius expression are 0.04 and 0.33 L mol^{-1} s^{-1} for the A and B channels, respectively. These values differ from the experimental values by several orders of magnitude because in the Arrhenius expression the activation energy is introduced in the exponential, and relatively small errors in the energies cause very large errors in the rate coefficients. They are mentioned here only to show that the rate coefficients of the two paths are similar and that both channels may be expected to occur.

The formation of the cyclic adduct may, in principle, also occur from the open adduct by the rotation of the nitrate group and a shortening of the O···C distance. In fact, to explain the observed formation of some simple aldehydes[10] Perez-Casany et al.[15−18] propose such a path. The transition state which separates the two isomeric forms, however, has an appreciable energy. For example, for propene, they obtain an energy barrier

TABLE 7: Activation Energies (in kcal/mol) for the NO_3 + Ethene Reaction, Calculated with Different Methods and Basis Sets[a]

	TS_{open}	TS_{cycle}	$TS_{open\rightarrow cycle}$
PMP2/6-31G**	21.47	19.74	30.11
PMP2/6-311G**	22.35	21.94	
CCSD(T)/6-311G** (SP)	12.65	9.49	24.36
B3LYP/6-31G**	−0.37		16.44
exptl	(5.72−6.21)		

[a] The PMP2/6-31G**, PMP2/6-311G**, and B3LYP/6-31G** results include ZPE at the corresponding levels. For the single point (SP) CCSD(T), the ZPE corrections are those from the MP2/6-31G** frequency calculation. The experimental activation energies are taken from refs 4, 6, and 7.

TABLE 8: Reaction Energies (in kcal/mol) at 298 K for the NO_3 + Ethene Reaction, Calculated with Different Methods and Basis Sets[a]

	ΔH_{open}	ΔH_{cycle}	$\Delta H_{open\rightarrow cycle}$
PMP2/6-31G**	−12.31	−17.02	−4.71
CCSD(T)/6-311G** (SP)	−20.97	−29.92	−8.95
B3LYP/6-31G**	−14.73	−27.78	−13.05

[a] The PMP2 and B3LYP results include TCE at the corresponding levels. For the SP CCSD(T) values, the TCE corrections are those from the MP2/6-31G** frequency calculation.

of 15.7 kcal/mol, calculated with the B3LYP method. If one takes into account the fact that the B3LYP method is well known to underestimate the size of activation barriers, this channel would not occur easily. We have calculated the corresponding barrier for ethene using B3LYP and other methods. The B3LYP/6-31G** result is 16.45 kcal/mol, with PMP2/6-31G** it is 30.11 kcal/mol, while at the CCSD(T)/6-311G**//MP2/6-31G** level, it is 24.36 kcal/mol. The MP2/6-31G** geometry of this transition state and its transition vector are shown in Figure 5, and the geometrical parameters are given in Table 5.

In view of the above discussion, we suggest the following mechanism for the initial reaction of NO_3 with ethene (Scheme 1):

The numbers indicated on the arrows are the CCSD(T) activation energies in kcal/mol.

In this mechanism, the reaction would occur, either by addition to one of the carbon atoms (path A), or by cycloaddition (path B). Path B has a much smaller frequency factor than path A, but its contribution could be significant because the energy of its transition state is lower than for path A. Also, the alternative way of forming the cyclic adduct from the open adduct involves a high energy isomerization process.

Once the adducts are formed, their fate depends on pressure and on whether oxygen is present or not. Four paths are proposed, and they are shown in Scheme 2:

Paths C and D occur in the absence of molecular oxygen. If NO_2 is present (path C), nitroxyethyl nitrate NEN is formed. In the case of propene, Bandow et al.[2] have found that NPN (which is the equivalent of NEN for propene) disappears as PGDN (equivalent to EGDN) is formed.

At low pressures, and according to the mechanism proposed by Perez-Casany et al. for the reaction of larger alkenes with NO_3 in an inert atmosphere,[15−18] cleavage of the cycle occurs (path D) to form NO and two aldehyde molecules (formaldehyde, in the case of ethene). In the absence of oxygen these products can only be obtained via the cyclic adduct.

In the presence of oxygen (path E), a nitrocarbonyl compound would be obtained.

Reaction with a hydrogenperoxyl radical, HO_2 (path F), would lead to the formation of a very stable cyclic compound (the reaction energy for path F, calculated at the PMP2/6-31G** level, is 103 kcal/mol).

The calculated total energies (in hartrees) for the NO_3 + ethene initial reaction at the PMP2/6-31G**, PMP2/6-311G**, CCSD(T)/6-311G**//MP2/6-31G** and B3LYP/6-31G** levels are given in Table 6 for both the cycloaddition and the open channels, and for the transition state connecting the two adducts. Zero point and thermal energy corrections are given at the levels indicated in Table.

Spin contamination is only significant at the transition states. Their $\langle S^2 \rangle$ values before projection range from about 0.8 to 1, and they reduce to 0.75 after projection.

The activation energies, including the ZPE corrections are given in kcal/mol in Table 7, together with experimental values. The activation energy of the transition state leading from the open adduct to the cyclic adduct, including the ZPE correction, is also given in Table 7. The large values obtained at all levels suggest that this pathway is not energetically favored.

Reaction energies, ($E_P - E_R$), at 298 K, for paths A and B, are given in Table 8 for the methods employed. The TCE corrections have been included in the energy differences. The cyclic adduct is always found to be considerably more stable than the open adduct. In fact, even at the B3LYP level, the cyclic adduct is 13 kcal/mol more stable than the open adduct.

All quantities necessary for the calculation of the preexponential factors along paths A and B are given in Table 9 using the partition functions obtained with various methods. Three and two low frequencies are present in the open addition and cycloaddition transition states, respectively, in addition to the imaginary frequency. Of these, two (for path A) and one (for path B) can be viewed as internal rotations. Thus, in the partition functions of the transition states, their harmonic contributions have been replaced by those of free rotors.[20]

4. Conclusion

Several methods based on different approaches to electron correlation have been used in this work to study the addition reaction of an NO_3 radical to ethene. Parallel to the accepted

TABLE 9: Partition Functions *Q* and Preexponential Factors *A* (in L mol^{-1} s^{-1}) for Paths A (Open Channel) and B (Cyclic Channel) of the NO_3 + Ethene Addition Reaction, Calculated at the MP2/6-31G, MP2/6-311G**, and B3LYP/6-31G** Levels[a]**

	method						
	MP2/6-31G**		MP2/6-311G**		B3LYP		
	path A	path B	path A	path B	path A	path B	exptl[b]
Q_{NO_3}	1.7732×10^{11}	1.7732×10^{11}	1.7075×10^{11}	1.7075×10^{11}	4.01×10^{11}	$4.01 \times 10^{1}1$	
Q_{ethene}	3.9788×10^{9}	3.9788×10^{9}	4.0351×10^{9}	4.0351×10^{9}	3.9934×10^{9}	3.9934×10^{9}	
Q_{TS}	5.6867×10^{13}	3.0065×10^{13}	5.9903×10^{13}	2.8802×10^{13}	6.24×10^{14}		
Q_{TS} corr	8.5709×10^{15}	3.4418×10^{14}	7.9465×10^{15}	3.3148×10^{14}	3.1175×10^{16}		
A	7.55×10^{7}	3.03×10^{6}	7.16×10^{7}	2.99×10^{6}	1.21×10^{8}		1.99×10^{9}

[a] The indicated partition functions have been corrected (Q_{TS} corr) for internal rotations (see text); the other values are those obtained from Gaussian98. [b] The experimental preexponential factor is given in L mol^{-1} s^{-1}.

mechanism of addition of NO_3 to one of the carbon atoms of the double bond, another addition channel is proposed, which is analogous to the one in ozone cycloaddition and which provides a low energy path yielding formaldehyde and NO as the final products. The results obtained at the single point CCSD(T)/6-311G**//MP2/6-31G** level for the calculated energy barriers agree best with the experimental value. The predicted Arrhenius parameters are reported.

From the results we conclude that, when the NO_3−alkene reaction occurs, a cycloaddition channel is possible, in which two of the oxygen atoms of the nitrate radical add simultaneously to the carbon atoms of the double bond. A very stable cyclic adduct is formed, which bears a striking resemblance to the primary ozonide obtained in the O_3 addition to ethene.[24] In fact, with seven electrons more than in the case of the primary ozonide, but with one electron localized outside of the ring system, the NO_3 + ethene cycloaddition could also be symmetry-allowed in the spirit of the $(4q + 2)$ Woodward−Hoffmann rules.[25] The cyclic adduct is at least 6 kcal/mol more stable than the open adduct.

No van der Waals complex seems to be formed previous to the addition transition states, and this can be explained in terms of the lack of a dipole moment in NO_3 in a D_{3h} conformation.

The energy difference between the cyclic and the open transition states varies with the method of calculation used. With either the MP2 or the CCSD(T) methods, the difference is about 3 kcal/mol, in favor of forming the cyclic adduct. Because the open transition state is unusually constrained and has a preexponential factor which is only about 1 order of magnitude larger than the one for cycloaddition, we expect that the rate constants for the two channels could be similar.

Work is in progress to calculate Arrhenius parameters for paths A and B in the reaction of NO_3 with a series of alkenes to see if the same competition could occur in other cases, and if the relative weights of the two channels explain the differences in the final products (aldehydes vs nitrate products) observed by Barnes et al.[10] for the reaction of different alkenes with NO_3.

The formation of formaldehyde and of NO as final products, in the absence of molecular oxygen, requires that a cyclic adduct intermediary be formed. Because the path that would allow the transformation of the open adduct into the cyclic adduct presents a high barrier, we suggest that the direct cycloaddition constitutes a significant alternative. Also, from this adduct radical, different channels are possible, depending on the pressure and the composition of the gaseous environment. Our MP2 calculations of the reaction profiles, both in the presence of oxygen and in anaerobic conditions, show that, from the nitroalkoxy radical, all the experimentally identified products can be obtained. Details of these calculations will be presented elsewhere.

Acknowledgment. The authors gratefully acknowledge the financial support from the Instituto Mexicano del Petróleo through program FIES-95-97-VI and the computing time on the Silicon Graphics Origin 2000 at the Universidad Nacional Autónoma de Mexico(UNAM). R. C. R. thanks CONACyT for a fellowship.

References and Notes

(1) Finlayson-Pitts, B. J.; Pitts, N. *Atmospheric Chemistry*: *Fundamentals and Experimental Techniques*; Wiley-Interscience; New York, 1986.

(2) Bandow, H.; Okuda, M.; Akimoto, H. *J. Phys. Chem*. **1980**, *84*, 3604.

(3) Shepson, P. B.; Edney, E. O.; Kleindienst, T. E.; Pittman, J. H.; Namie, G. R.; Cupitt, L. T. *Environ. Sci. Technol*. **1985**, *18*, 849.

(4) Atkinson, R. *J. Phys. Chem. Ref. Data* **1997**, *26*, 215.

(5) Martinez, E.; Cabañas, B.; Aranda, A.; Martín, P.; Salgado, S. *Int. J. Chem. Kinet.* **1997**, *29*, 927.

(6) Wayne, R. P.; Barnes, I.; Biggs, P.; Burrows, J. P.; Canosa-Mas, C. F.; Hjorth, J.; Bras, G. L.; Moortgat, G. K.; Perner, D.; Poulet, G.; Restelli, G.; Gidebottom, I. *Atmos. Environ*. **1991**, *35A*, 1.

(7) *The NIST Chemical Kinetics Data Base*; NIST Standard Reference Database 17-2Q98. National Institutes of Standards and Technology: Washington, DC.

(8) Morrison, R. T.; Boyd, R. N. *Organic Chemistry*; Allyn and Bacon, Inc.; Boston, 1983.

(9) Dlugokencky, E. J.; Howard, C. J. *Phys. Chem*. **1989**, *93*, 1091.

(10) Barnes, I.; Bastian, V.; Becker, K. H.; Tong, Z. *Phys. Chem*. **1990**, *94*, 2413.

(11) Skov, H.; Benter, T.; Schindler, R. N.; Hjorth, J.; Restelli, G. *Atmos. Environ*. **1994**, *28*, 1583.

(12) Berndt, T.; Böge, O. *Ber. Bunsen-Ges. Phys. Chem*. **1994**, *98*, 869.

(13) Berndt, T.; Böge, O. *J. Atmos. Chem*. **1995**, *21*, 275.

(14) Pérez-Casany, M. P.; Nebot-Gil, I.; Sánchez-Marín, J.; Tomás-Vert, F. *J. Org. Chem*. **1998**, *63*, 6978.

(15) Pérez-Casany, M. P.; Nebot-Gil, I.; Sánchez-Marín, J. *J. Phys. Chem. A* **2000**, *104*, 6277.

(16) Pérez-Casany, M. P.; Nebot-Gil, I.; Sánchez-Marín, J. *J. Phys. Chem. A* **2000**, *104*, 10721.

(17) Pérez-Casany, M. P.; Nebot-Gil, I.; Sánchez-Marín, J. *J. Am. Chem. Soc*. **2000**, *122*, 11585.

(18) Pérez-Casany, M. P.; Nebot-Gil, I.; Sánchez-Marín, J. *J. Phys. Chem. A* **2000**, *104*, 11340.

(19) Frisch, M. J.; Trucks, G. W.; Schlegel, H. B.; Gill, P. M. W.; Johnson, B. G.; Robb, M. A.; Cheeseman, J. R.; Keith, T. A.; Petersson, G. A.; Montgomery, J. A.; Raghavachari, K.; Al-Laham, M. A.; Zakrzewski, V. G.; Ortiz, J. V.; Foresman, J. B.; Cioslowski, J.; Stefanov, B. B.; Nanayakkara, A.; Challacombe, M.; Peng, C. Y.; Ayala, P. Y.; Chen, W.; Wong, M. W.; Andres, J. L.; Replogle, E. S.; Gomperts, R.; Martin, R. L.; Fox, D. J.; Binkley, J. S.; Defrees, D. J.; Baker, J.; Stewart, J. P.; Head-Gordon, M.; Gonzalez, C.; Pople, J. A. *Gaussian94*; Gaussian, Inc.; Pittsburgh, PA, 1995.

(20) Benson, S. W. *Thermochemical Kinetics*; Wiley and Sons: New York; 1976; p 43.

(21) Sosa, C.; Schlegel, H. B. *J. Am. Chem. Soc.* **1987**, *109*, 4193.

(22) Díaz-Acosta, I.; Alvarez-Idaboy, J. R.; Vivier-Bunge, A. *Int. J. Chem. Kin*. **1999**, *31*, 29.

(23) Sekušak, S.; Liedl, K. R.; Sabljić, A. J. *Phys. Chem. A* **1998**, *102*, 1583.

(24) Anglada, J. M.; Crehuet, R.; Bofill, J. M. *Chem. Eur. J*. **1999**, *5*, 1809.

(25) Woodward, R. B.; Hoffmann, R. *The Conservation of Orbital Symmetry*; Verlag Chemie Academic Press: Berlin, 1971; p 70.

(26) Gillies, C. W.; Gillies, J. Z.; Suenram, R. D.; Lovas, F. J.; Kraka, E.; Cremer, D. *J. Am. Chem. Soc*. **1991**, *113*, 2412.

(27) Alvarez-Idaboy, J. R.; Diaz-Acosta, I.; Vivier-Bunge, A. *J. Comput. Chem*. **1998**, *88*, 811.

(28) Uc, V. H.; García-Cruz, I.; Vivier-Bunge, A. *Quantum Systems in Chemistry and Physics*; Hernández-Laguna, A., et al., Eds.; Kluwer Academic Publishers: Great Britain, 2000; Vol. II, p 241.

(29) Alvarez-Idaboy, J. R.; Mora-Diez, N.; Vivier-Bunge, A. *J. Am. Chem. Soc*. **2000**, *122*, 3715.

(30) Uc, V. H.; García-Cruz, I.; Hernández-Laguna, A.; Vivier-Bunge, A. *J. Phys. Chem*. **2000**, *104*, 7847.

(31) Atkinson, R. *Chem. Rev*. **1986**, *86*, 69.

(32) Canosa-Mas, C.; Smith, S. J.; Toby, S.; Wayne, R. P. *J. Chem. Soc., Faraday Trans*. **1988**, *88*, 247.